

An Analysis of the Isomerization Energies of 1,2-/1,3-Diazacyclobutadiene, Pyrazole/Imidazole, and Pyridazine/Pyrimidine with the Turn-Upside-Down Approach

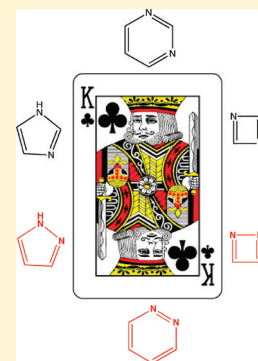
Majid El-Hamdi,[†] William Tiznado,[‡] Jordi Poater,^{*,†} and Miquel Solà^{*,†}

[†]Institut de Química Computacional and Departament de Química, Universitat de Girona, Campus Montilivi, E-17071 Girona, Catalonia, Spain

[‡]Departamento de Ciencias Químicas, Facultad de Ciencias Exactas, Universidad Andres Bello, Avenida República 275, Santiago de Chile, Chile

Supporting Information

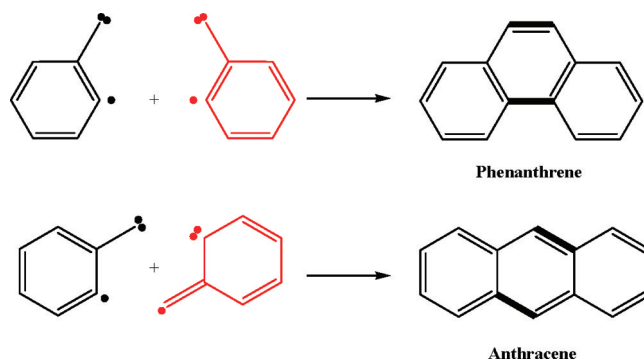
ABSTRACT: The isomerization energies of 1,2- and 1,3-diazacyclobutadiene, pyrazole and imidazole, and pyridazine and pyrimidine are 10.6, 9.4, and 20.9 kcal/mol, respectively, at the BP86/TZ2P level of theory. These energies are analyzed using a Morokuma-like energy decomposition analysis in conjunction with what we have called turn-upside-down approach. Our results indicate that, in the three cases, the higher stability of the 1,3-isomers is not due to lower Pauli repulsions but because of the more favorable σ -orbital interactions involved in the formation of two C–N bonds in comparison with the generation of C–C and N–N bonds in the 1,2-isomers.



1. INTRODUCTION

The isomerization energy is the energy difference between two isomers, i.e., the energetic cost corresponding to the transformation of a molecule into another, both having the same number and type of atoms but rearranged in different manner. In many cases, both structural and stereoisomers can be constructed from the same fragments but just connecting the two fragments in different ways. This is the case, for instance, of phenanthrene and anthracene, the kinked phenacene and linear acene isomers of molecular formula $C_{14}H_{10}$ that can be made from two identical 2-methtriylphenyl fragments (i.e., $C_6H_4 \cdot \text{CH}^{\bullet\bullet} + C_6H_4 \cdot \text{CH}^{\bullet\bullet}$) as shown in Scheme 1.¹ By just turning upside down the red fragment in Scheme 1 (two resonant structures for the same 2-methtriylphenyl fragment are depicted in red) one builds the two different isomers from identical fragments. The bonding energy for the formation of each isomer from the same fragments can then be analyzed using a Morokuma-like energy decomposition analysis (EDA)² or by any other method to decompose the bonding energy. From this analysis, one can get a deeper insight into the origin of the isomerization energy. This method of analysis, for which we propose the name turn-upside-down approach, was used some years ago¹ to show that the higher stability of phenanthrene with respect to anthracene is due to the more efficient bonding in the π -electron system and not to H–H bonding interactions between the two hydrogen atoms in the

Scheme 1. Formation of Structural Isomers Anthracene and Phenanthrene from Two Identical 2-Methtriylphenyl Fragments



bay region of phenanthrene as proposed by Matta and co-workers.³ More recently, other authors have provided experimental support to the thesis that there is H–H steric repulsion, not H–H bonding, between the bay hydrogen atoms of phenanthrene.⁴

Aromatic and antiaromatic diaza-substituted compounds are obtained after double substitution of CH groups in classical

Received: August 9, 2011

Published: September 27, 2011

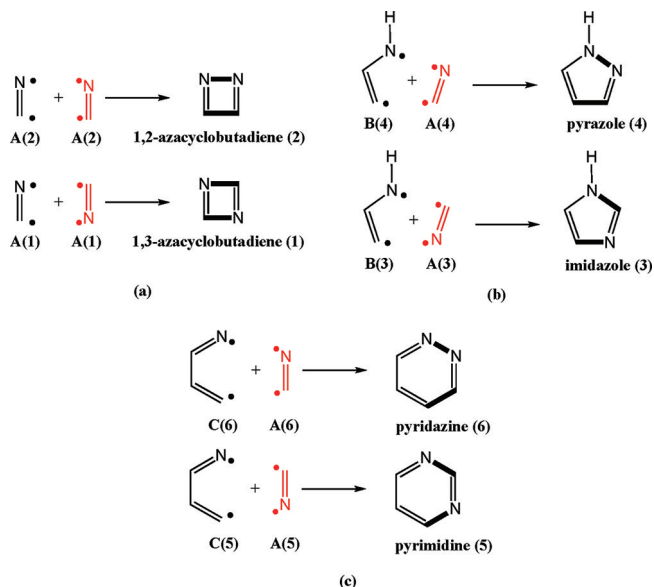
organic (anti)aromatic species by N atoms.⁵ Among the simplest diaza-substituted compounds one finds the antiaromatic 1,2- and 1,3-diazacyclobutadiene species. Although these two structural isomers have not been synthesized yet, except for some substituted analogues,⁶ they have been postulated as possible intermediates in reaction mechanisms of several photochemical processes.⁷ In addition, the related 1,2-diphosphocyclobutadiene unit has been recently observed in 1,2,4-triphosphaferrocenes.⁸ Politzer et al.⁹ reported that these antiaromatic rings could be stabilized with π -donor substituents such as amino groups. The substitution of CH groups in pyrrole by N atoms results in the formation of azoles. Monosubstitution leads to 1,2- (pyrazoles) and 1,3-azoles (imidazoles). Derivatives of pyrazoles and of their either reduced (pyrazolines) or oxidized (pyrazolones) forms are present in many pharmaceutical drugs and have antibacterial and antifungal properties.^{10,11} On the other hand, the imidazole ring is the building block of many important biological compounds such as histidine. Moreover, substituted imidazoles and imidazole derivatives are also present in fungicides and many medications.¹⁰ On the other hand, the most relevant diaza-substituted compounds are probably the diazabenzene species that have three structural isomers, namely, 1,2-diazabenzene (pyridazine), 1,3-diazabenzene (pyrimidine), and 1,4-diazabenzene (pyrazine). Pyridazine is employed in the synthesis of intermediates used in the production of insecticides and herbicides, and it can also be found within the structure of several medicines. Pyrimidine is the building block of nucleic acid pyrimidine bases and, linked to an heteroaromatic five-membered ring (5-MR), of purine bases.¹⁰

1,2-Diazabenzene and -cyclobutadiene and pyrazole with two adjacent nitrogen atoms are less stable than the corresponding 1,3-isomers. Standard enthalpies of formation indicate that pyrimidine and imidazole are more stable than pyridazine and pyrazole by about 20^{12,13} and 10^{14–16} kcal/mol, respectively. On the other hand, previous MNDO calculations also favored the 1,3- with respect to the 1,2-diazacyclobutadiene by 32.6 kcal/mol.¹⁷ Lone-pair repulsion in NN bonds is the usual explanation for the lower stabilities of the NN isomers.^{18,19} However, lone-pair protonation and diprotonation of pyridazine and pyrimidine barely change its energy difference.²⁰ Therefore, it seems that lone-pair repulsion cannot be the only cause that explains the higher stability of 1,3-isomers. Although the strength of the N=N π -bond is somewhat lower than that of the C=C and C=N bonds, the difference of about 6 kcal/mol²⁰ is not enough to explain the relative energies of 1,2- and 1,3-diaza and azole compounds either. Therefore, the reason for the lower stability of 1,2-diazabenzene and -cyclobutadiene and pyrazole in comparison to their 1,3-counterparts has to be attributed in part to the σ -skeleton,²⁰ and it is not fully understood yet. The goal of this work is to carry out a detailed analysis of the isomerization energy of these 1,2- and 1,3-isomers with the so-called turn-upside-down approach (see Scheme 2) with the aim of providing a better comprehension on the origin of the NN bond destabilization.

2. THEORETICAL METHODS

2.1. General Procedure. All density functional theory (DFT) calculations were performed with the Amsterdam Density Functional (ADF) program.^{21,22} The molecular orbitals (MOs) were expanded in a large uncontracted set of Slater type orbitals (STOs) of triple- ζ quality for all atoms including two sets of polarization functions (2p and 3d on H and 3d and 4f on

Scheme 2. Formation of (a) 1,2- and 1,3-Diazacyclobutadiene, (b) Pyrazole/Imidazole, and (c) Pyridazine/Pyrimidine Structural Isomers from Two Triplet Biradical Fragments with the Turn-Upside-Down Approach



C and N).²³ The 1s core electrons of carbon and nitrogen were treated by the frozen core approximation²² as it was shown to have a negligible effect on the obtained geometries.²⁴ An auxiliary set of s, p, d, f, and g STOs was used to fit the molecular density and to represent the Coulomb and exchange potentials accurately for each SCF cycle.²⁵ Energies and gradients were computed using the local density approximation (Slater exchange and VWN correlation)²⁶ with nonlocal corrections for exchange (Becke88)²⁷ and correlation (Perdew86)²⁸ included self-consistently (i.e., the BP86 functional).

Analytical Hessians were computed to confirm the nature of the located minima. Bond enthalpies and Gibbs energies at 298.15 K and 1 atm (ΔH and ΔG) were calculated from electronic bond energies (ΔE) and frequency computations using standard statistical-mechanics relationships for an ideal gas.²⁹

Isomerization energies were also calculated with the Gaussian 09 program³⁰ at the coupled cluster level³¹ with single and double excitations (CCSD)³² and with triple excitations treated perturbatively (CCSD(T))³³ using the Dunning's correlation consistent augmented triple- ζ (aug-cc-pVTZ) basis set for nitrogen, carbon, and hydrogen³⁴ at the optimized BP86/TZ2P molecular geometries.

2.2. Bond Energy Decomposition. The bonding energy corresponding to the formation of a given aza compound from two triplet biradicals, fragment 1 ($\alpha\alpha$) + fragment 2 ($\beta\beta$) (see Scheme 2), is made up of two major components (eq 1):

$$\Delta E = \Delta E_{\text{prep}} + \Delta E_{\text{int}} \quad (1)$$

In this formula, the preparation energy ΔE_{prep} is the amount of energy required to deform the separated biradical fragments in their triplet state from their equilibrium structure to the geometry that they acquire in the cyclic molecule. The interaction energy ΔE_{int} corresponds to the actual energy change when the prepared fragments are combined to form the overall molecule. It is analyzed in the framework of the Kohn–

Sham MO model using a Morokuma-type decomposition of the bonding energy into electrostatic interaction, exchange (or Pauli) repulsion, and orbital interactions (eq 2).^{2,35,36}

$$\Delta E_{\text{int}} = \Delta V_{\text{elstat}} + \Delta E_{\text{Pauli}} + \Delta E_{\text{oi}} \quad (2)$$

The term ΔV_{elstat} corresponds to the classical electrostatic interaction between the unperturbed charge distributions of the prepared (i.e., deformed) fragments and is usually attractive. The Pauli repulsion ΔE_{Pauli} comprises the destabilizing interactions between occupied orbitals. It arises as the energy change associated with going from the superposition of the unperturbed electron densities of the two fragments to the wave function $\Psi^0 = N A [\Psi_{\text{fragment1}}^{\alpha\alpha} \Psi_{\text{fragment2}}^{\beta\beta}]$, that properly obeys the Pauli principle through explicit antisymmetrization (A operator) and renormalization (N constant) of the product of fragment wave functions. It comprises the four-electron destabilizing interactions between occupied MOs and is responsible for the steric repulsion. The orbital interaction ΔE_{oi} is the change in energy from Ψ^0 to the final, fully converged wave function Ψ_{SCF} of the system. The orbital interactions account for charge transfer (i.e., donor–acceptor interactions between occupied orbitals on one fragment with unoccupied orbitals of the other, including the HOMO–LUMO interactions) and polarization (empty–occupied orbital mixing on one fragment due to the presence of another fragment). The ΔE_{oi} term can be divided into contributions of orbitals having different symmetry (eq 3) using the extended transition state (ETS) scheme developed by Ziegler and Rauk.³⁶

$$\Delta E_{\text{oi}} = \sum_{\Gamma} \Delta E_{\Gamma} \quad (3)$$

In the present planar systems with a clear σ/π separation, this symmetry partitioning proved to be very useful. In the bond-energy decomposition, open-shell fragments were treated with the spin-unrestricted formalism, but for technical reasons, spin-polarization was not included. This error causes the studied bond to become in the order of a few kcal/mol too strong. To facilitate a straightforward comparison, the EDA results were scaled to match exactly the regular bond energies (the correction factor is consistently in the range 0.96–0.97 in all model systems and does therefore not affect trends). A similar scheme based in the same EDA approach was used by Frenking and co-workers to estimate the strength of π -cyclic conjugation in typical aromatic and antiaromatic organic compounds³⁷ and in metallabenzenes.³⁸

3. RESULTS AND DISCUSSION

This section is divided into three subsections, each of them devoted to one of the three pairs of cyclic azaisomers analyzed in this paper.

3.1. 1,2- and 1,3-Diazacyclobutadiene. The geometries of the closed-shell singlet ground state of 1,2- and 1,3-diazacyclobutadiene are depicted in Figure 1 (Cartesian coordinates are given in the Supporting Information.) The molecular structures of 1,2- and 1,3-diazacyclobutadiene are close to those reported by Jursic³⁹ at the MP2/6-31G(d) and B3LYP/6-311G(2d,2p) levels and Politzer et al.⁹ with the HF/3-21G method, respectively. The molecular structure of 1,2-diazacyclobutadiene indicates that the π -electrons are localized in the C=N bonds. In line with this result, the sum of the G3 bond energies recently reported by Wang and co-workers²⁰

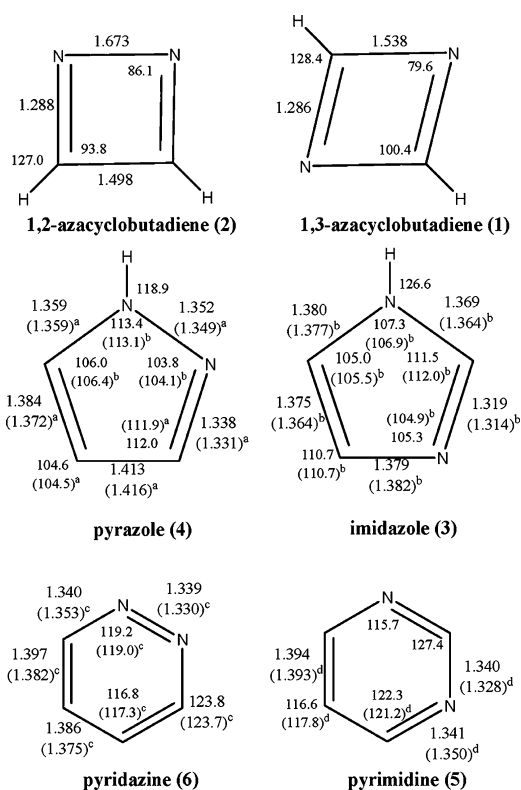


Figure 1. Geometries (in Å, deg) of the studied diaza compounds computed at BP86/TZ2P. Experimental values are given in parentheses. Key: (a) from ref 48; (b) from ref 49; (c) from ref 61; (d) From ref 62.

shows that the configuration with C–C, N–N, and two C=N bonds is 5.2 kcal/mol more stable than the arrangement with C=C, N=N, and two C–N bonds. The N–N bond in the 1,2-diazacyclobutadiene is almost broken (1.673 Å). We have checked that the optimization of the open-shell singlet species leads to the closed-shell singlet state, and therefore, the closed-shell singlet is the ground state for this species. BP86/TZ2P results show that the lowest lying aromatic triplet state for the two isomers is 17.89 and 20.33 kcal/mol higher in energy for 1,2- and 1,3-diazacyclobutadiene, respectively. The antiaromaticity of the singlet ground state of these two isomers is supported by the positive values of the NICS indicator of aromaticity⁴⁰ (1,2-diazacyclobutadiene: NICS(1) = 11.2 ppm and NICS(1)_{zz} = 4.3 ppm; 1,3-diazacyclobutadiene: NICS(1) = 12.0 ppm and NICS(1)_{zz} = 43.1 ppm), the large aromatic fluctuation index⁴¹ (1,2-diazacyclobutadiene: FLU = 0.179; 1,3-diazacyclobutadiene: FLU = 0.148), and the negative value of the electronic delocalization multicenter index^{42,43} (1,2-diazacyclobutadiene: MCI = –0.001; 1,3-diazacyclobutadiene: MCI = –0.013). This situation is similar to that found in cyclobutadiene.^{9,44}

As can be seen in Table 1, the 1,3-diazacyclobutadiene isomer is about 10–11 kcal/mol more stable than the 1,2-diazacyclobutadiene, the BP86/TZ2P and CCSD(T)/aug-cc-pVTZ//BP86/TZ2P methods differing by less than half of a kcal/mol. The higher stability of 1,3- with respect to 1,2-diazacyclobutadiene was already predicted (although clearly overestimated) with semiempirical MNDO calculations.¹⁷

To understand the origin of the higher stability of 1,3-diazacyclobutadiene (1) in comparison with its 1,2-diazacyclobutadiene (2) isomer, we have analyzed the formation of 1 and

Table 1. Isomerization Energies, Enthalpies, And Gibbs Energies of the Three Pairs of Isomers Considered in This Study (Units are kcal/mol)^a

isomers	ΔE		ΔH		ΔG
	BP86/TZ2P	CCSD(T)/aug-cc-pVTZ ^b	BP86/TZ2P	expt	BP86/TZ2P
1,2-/1,3-diazacyclobutadiene	10.62	10.91	10.57		10.55
pyrazole/imidazole	9.36	10.84	9.41	12.7 ± 3.9 ^c 11.1 ± 0.3 ^d	9.41
pyridazine/iyrimidine	20.89	22.68	20.72	19.7 ^e	20.38

^aThe most stable isomers are 1,3-diazacyclobutadiene, imidazole, and pyrimidine. ^bFrom single-point energy calculations at the BP86/TZ2P-optimized geometries. ^cFrom heats of combustion of ref 14. ^dFrom heats of combustion of ref 15. ^eFrom heats of combustion of ref 12.

Table 2. Analysis of the Bonding (in kcal/mol) between Two Triplet Azaethendiyl Fragments (A) in 1,3-Diazabutadiene (1), 1,2-Diazabutadiene (2), and Deformed 1,2-Diazabutadienes (2a and 2b)^a

	1	2	2a	2b
	A(1) + A(1)	A(2) + A(2)	A(1) + A(1)	A(1) + A(1)
ΔE_{Pauli}	425.81	344.71 (−81.10)	413.86 (−11.95)	362.53 (−63.28)
ΔV_{elstat}	−220.89	−189.47 (31.41)	−208.73 (12.15)	−194.89 (26.00)
ΔE_{σ}	−364.37	−305.75 (58.63)	−338.51 (25.87)	−305.52 (58.86)
ΔE_{π}	−13.58	−10.04 (3.54)	−11.23 (2.35)	−11.02 (2.56)
ΔE_{oi}	−377.95	−315.79 (62.16)	−349.74 (28.21)	−316.54 (61.42)
ΔE_{int}	−173.02	−160.55 (12.47)	−144.61 (28.42)	−148.89 (24.13)
ΔE_{def}	3.54	1.69 (−1.85)	3.54 (0.00)	3.54 (0.00)
ΔE	−169.48	−158.86 (10.62)	−141.07 (28.41)	−145.35 (24.13)

^aComputed at BP86/TZ2P. See Figure 1 for structures. A(1) and A(2) refer to A in the geometry it adopts in 1 and 2, respectively; 2a is 1,2-diazacyclobutadiene with frozen A(1) fragments but with connecting N–N and C–C bond distances as the corresponding C–N bond lengths in 1 (1.538 Å); 2b is 1,2-diazacyclobutadiene with frozen A(1) fragments but with connecting N–N and C–C bond distances as the optimized bond lengths in 2. Values in parentheses show the difference of the energy term with the corresponding one for 1 from A(1) + A(1).

2 from two identical azaethendiyl fragments A in their triplet states. The azaethendiyl fragments that can be obtained from 1 and 2 are slightly different (C–N bonds are 1.286 and 1.288 Å, and $\angle\text{HCN}$ angles are 131.2 and 127.0°, respectively), and therefore, one can build 1 and 2 using azaethendiyl fragments derived from 1, the so-called A(1) fragment, or originated from 2 (A(2), see Scheme 2).

Construction of 1 or 2 from A involves the formation of two new σ -electron pairs (two new C–N bonds in 1 and C–C and N–N bonds in 2) plus the rearrangement of the π -system that becomes partially delocalized. Table 2 contains the results of the analysis of the bonding for 1,3-diazacyclobutadiene, 1,2-diazacyclobutadiene, and two deformed 1,2-diazacyclobutadiene structures (2a and 2b). As can be seen, 169.5 and 158.9 kcal/mol are released in the formation of 1 from two A(1) fragments and 2 from two A(2) fragments, respectively, thus giving 1 as the most stable isomer by 10.6 kcal/mol. The higher stability of 1 cannot be ascribed to the deformation energy of the fragments (ΔE_{def}) that is in fact somewhat more destabilizing for fragment A(1) than A(2). The main difference comes from the interaction energy (ΔE_{int}) that is 12.5 kcal/mol more stabilizing in 1. The EDA results of these two ΔE_{int} energies show that the difference is not due to Pauli repulsions (ΔE_{Pauli}) that stabilize 2 with respect to 1 by as much as 81.1 kcal/mol but to a combination of better electrostatic (ΔV_{elstat}) and orbital interaction (ΔE_{oi}) components. Therefore, higher vicinal NN lone-pair repulsion is compensated by the low Pauli repulsion of the CC bond and, therefore, cannot be used as the only explanation for the lower stability of the 1,2-diazacyclobutadiene isomer. The more stabilizing ΔV_{elstat} term in the 1,3-diazacyclobutadiene form is easily understood by taking into account that in this isomer the dipole moments of the azaethendiyl fragments are better oriented to favor the

electrostatic interactions. The ΔE_{oi} can be further decomposed into σ and π components (ΔE_{σ} and ΔE_{π}). Both favor the 1,3-diazacyclobutadiene isomer, although the main contribution (58.6 kcal/mol) comes from the σ -system. The π -component, which measures the contribution of π -delocalization to the bonding energy (in fact, it may be considered as an approximation to the Hückel resonance energy⁴⁵), is in both isomers quite low as expected for antiaromatic species. The lower π -interaction energy in 1,2-diazacyclobutadiene can be ascribed in part to the larger N–N bond length that makes π -delocalization somewhat less efficient. Thus, what is more remarkable is the large difference in the ΔE_{σ} component.

To analyze this aspect in more detail we have made EDAs of the eclipsed conformations of ethane, methylamine, and *cis*-hydrazine, and we have depicted the changes in the different energy components when going from 1.3 to 5 Å using the geometries of the fragments corresponding to the optimized geometry of these species (no reoptimization of the systems has been carried out). The results are summarized in Figures S1 and S2 of the Supporting Information. The C–C bond has the largest strength followed by the C–N and N–N bonds. The comparatively larger dissociation energy of the C–C bond can be attributed basically to its lower Pauli repulsion. In fact, the trend in bond strength follows the opposite tendency of the Pauli repulsion that increases along the series C–C < C–N < N–N. As it is usually the case,⁴⁶ larger Pauli repulsion goes with more favorable electrostatic interactions and, therefore, electrostatics favors the N–N bond followed by the C–N and C–C bonds. The same tendency remains for the orbital interactions despite the fact that the two SOMOs of the methyl radicals have much more favorable overlap and Fock matrix elements ($\langle\sigma_{\text{SOMO}}|F|\sigma_{\text{SOMO}}\rangle$). The less stabilizing orbital interactions (ΔE_{oi}) in the C–C bond as compared to the

Table 3. Analysis of the Bonding (in kcal/mol) between Triplet Azaethenediyl Fragment (A) and Triplet 1-Azapropenediyl (B) in Imidazole (3), Pyrazole (4), and Deformed Pyrazoles (4a and 4b)^a

	3	4	4a	4b
	A(3) + B(3)	A(4) + B(4)	A(3) + B(3)	A(3) + B(3)
ΔE_{Pauli}	621.48	593.31 (−28.17)	610.06 (−11.43)	603.88 (−17.60)
ΔV_{elstat}	−338.50	−329.53 (8.97)	−335.45 (3.05)	−330.17 (8.33)
ΔE_{σ}	−499.06	−468.81 (30.25)	−471.43 (27.63)	−471.97 (27.10)
ΔE_{π}	−66.49	−67.10 (−0.61)	−66.65 (−0.16)	−64.04 (2.45)
ΔE_{oi}	−565.55	−535.92 (29.63)	−538.08 (27.47)	−536.01 (29.54)
ΔE_{int}	−282.58	−272.13 (10.45)	−263.48 (19.10)	−262.31 (20.27)
ΔE_{def}	21.72	20.63 (−1.09)	21.72 (0.00)	21.72 (0.00)
ΔE	−260.86	−251.50 (9.36)	−241.76 (19.10)	−240.59 (20.27)

^aComputed at BP86/TZ2P. See Figure 1 for structures. A/B(3) and A/B(4) refer to A and B in the geometry they adopt in 3 and 4, respectively; 4a is pyrazole with frozen A(3) and B(3) fragments but with connecting (H)N–N and C–C bond distances as the corresponding C–N bond lengths in 3; 4b is pyrazole with frozen A(3) and B(3) fragments but with connecting (H)N–N and C–C bond distances as the optimized bond lengths in 4. Values in parentheses show the difference of the energy term with the corresponding one for 3 from A(3) + B(3).

N–N bond has to be attributed, on one hand, to the higher Pauli repulsion between the bond pair formed and the 2s electrons in ethane and, on the other hand, to the polarization of the 2s and lone-pair electrons into the N–N antibonding orbital of hydrazine (both effects are embodied in the orbital interaction term and are favored by the high C–C and low N–N overlaps) as discussed by Bickelhaupt et al.⁴⁷ in their analysis of the C–C, C–N, and N–N bond formation from two CN• radicals. The C–N bond in methylamine represents an intermediate situation. Because of C–C and N–N bond strength differences, the C–C bond length and the $\angle\text{NNC}$ angle in 2 are smaller than the N–N and the $\angle\text{CCN}$ ones. Finally, we note in passing that in a previous study it was reported that the reason for the C–C bond in CH₃–CH₃ being stronger than the C–N bond in CH₃–NH₂ is the relief in Pauli repulsion associated with the pyramidalization of the methyl group that compensates the strain energy needed to pyramidalize the methyl radical.⁴⁶

This is the situation at the optimized geometries of 1 and 2. It may happen, however, that the lower Pauli in 2 is due to the long N–N bond. In this case, the Pauli repulsion due to the NN lone-pair repulsion would have a decisive role in the final geometry and total energy of 1,2-diazacyclobutadiene. To analyze this point we have made an EDA of a deformed 1,2-diazacyclobutadiene (2a) generated from A(1) fragments but with connecting N–N and C–C bond distances equal to the corresponding C–N bond lengths in 1. In this way, 1 and 2a are exactly the same compound but just with an A(1) fragment turned upside down in 2a. Not surprisingly, the energy difference between the two isomers now increases to 28.4 kcal/mol. Interestingly, although the Pauli repulsion increases significantly from 2 to 2a, even in 2a the Pauli repulsion is somewhat smaller (12.0 kcal/mol) than in 1. So, definitely, the higher Pauli repulsion due to NN lone-pair repulsion in NN is compensated by the low Pauli repulsion of the C–C bond and is not the responsible of the lower stability of 1,2-diazacyclobutadiene. Not unexpectedly, the ΔV_{elstat} and ΔE_{oi} terms become more stabilizing in 2a as compared to 2 due to the shorter N–N distance. The change in the ΔE_{oi} term is almost entirely due to the ΔE_{σ} component, ΔE_{π} remaining almost unchanged. As a whole, the more favorable ΔV_{elstat} and ΔE_{oi} terms are compensated by a larger Pauli repulsion that makes 2a less stable than 2 as could be anticipated from the fact that the latter corresponds to the optimized geometry of 1,2-diazacyclobutadiene. Finally, we move from 2a to 2b, the latter

being a deformed 1,2-diazacyclobutadiene generated from A(1) fragments but with connecting N–N and C–C bond distances equal to the corresponding bond lengths in 2. Unsurprisingly, when going from 2a to 2b there is an important reduction of the Pauli repulsion term due to the longer N–N bond and a reduction of the ΔV_{elstat} and ΔE_{oi} terms, the latter coming almost exclusively from the ΔE_{σ} component. As a whole, 2b is 4.3 kcal/mol more stable than 2a.

3.2. 1,2- and 1,3-Azoles. The BP86/TZ2P geometries of the closed-shell singlet ground state of the pyrazole and imidazole rings are depicted in Figure 1 (Cartesian coordinates are given in the Supporting Information). Their molecular structures are very close to the experimental values obtained from microwave spectroscopy by Nygaard et al.⁴⁸ and Christen and co-workers,⁴⁹ respectively, differences in CC, NN, and CN bond lengths being less than one hundredth of an angstrom and in the angles of one tenth of a degree. Interestingly, in pyrazole the $\angle\text{HNN}$ angle (118.9°) is smaller than the $\angle\text{HNC}$ angle (126.6°) in imidazole due to the partial intramolecular hydrogen bond (H-bond) interaction between the H atom of the NH group and the lone pair of N in pyrazole.⁵⁰ As can be seen in Table 1, imidazole is about 9–11 kcal/mol more stable than pyrazole at the BP86/TZ2P and CCSD(T)/aug-cc-pVTZ//BP86/TZ2P levels of theory, not far from the experimental values determined from their enthalpies of combustion.^{14,15} The reason for this energy difference is not due to aromaticity. In general, most of the methods used to estimate the aromaticity of the pyrazole and imidazole rings point out that the two rings have similar aromaticity. This is the result one obtains with aromaticity descriptors such as resonance energies,^{14,18,19,51} aromatic stabilization energies,^{50–53} HOMA,^{16,50,52,54} HOSE,⁵⁴ Bird index,^{18,54,55} NICS,^{16,52} exaltation of magnetic susceptibility,⁵³ FLU,¹⁶ multicenter electronic indices,^{16,42,56} and analyzing the occupancy of the 2p_z orbitals.⁵⁷ Most of these indices indicate that the pyrazole ring is marginally more aromatic than the imidazole one. Only multicenter electronic indices^{16,58} (and not in all cases⁴²) and some resonance energies⁵¹ find imidazole slightly more aromatic than pyrazole. This is another example that the most aromatic isomer is not necessarily the most stable one.^{56,59} Moreover, it is an additional indication that in aromatic cycles with two or more N atoms the most aromatic ring is that having the largest number of NN units (or the smallest number of polarized CN bonds).^{54,56,60}

Table 4. Analysis of the Bonding (in kcal/mol) between the Triplet Azaethenediyl Fragment (A) and Triplet 1-Azabutenediyl (C) in Pyrimidine (5), Pyridazine (6), and Deformed Pyridazines (6a and 6b)^a

	5	6	6a	6b
	A(5) + C(5)	A(6) + C(6)	A(5) + C(5)	A(5) + C(5)
ΔE_{Pauli}	814.08	735.75 (−78.33)	789.47(−24.61)	756.25 (−57.83)
ΔV_{elstat}	−405.60	−373.10 (32.50)	−394.63 (10.97)	−379.47 (26.13)
ΔE_{σ}	−580.98	−519.59 (61.39)	−538.10 (42.87)	−530.18 (50.80)
ΔE_{π}	−79.03	−72.31 (6.72)	−79.99 (−0.95)	−72.89 (6.14)
ΔE_{oi}	−660.01	−591.91 (68.11)	−618.09 (41.92)	−603.07 (56.94)
ΔE_{int}	−251.53	−229.26 (22.27)	−223.25 (28.28)	−226.29 (25.24)
ΔE_{def}	16.44	15.06 (−1.38)	16.44 (0.00)	16.44 (0.00)
ΔE	−235.09	−214.20 (20.89)	−206.81 (28.28)	−209.85 (25.24)

^aComputed at BP86/TZ2P. See Figure 1 for structures. A/C(5) and A/C(6) refer to A and C in the geometry they adopt in 5 and 6, respectively; 6a is pyridazine with frozen A(5) and C(5) fragments but with connecting N–N and C–C bond distances as the corresponding C–N bond lengths in 5; 6b is pyridazine with frozen A(5) and C(5) fragments but with connecting N–N and C–C bond distances as the optimized bond lengths in 6. Values in parentheses show the difference of the energy term with the corresponding one for 5 from A(5) + C(5).

To get insight into the origin of the higher stability of imidazole (3) in comparison with pyrazole (4), we have analyzed their formation from azaethenediyl A and 1-azapropendiyl B fragments, both in their triplet states. The fragments A and B that can be obtained from 3 and 4 are slightly different and, therefore, 3 and 4 can be generated using fragments derived from 3, the so-called A(3) and B(3) fragments, or originated from 4 (A(4) + B(4)); see Scheme 2). The results of the EDA are given in Table 3.

The deformation energy of the fragments (ΔE_{def}) is somewhat less destabilizing for fragments A(4) + B(4) than A(3) + B(3), and therefore, this component does not explain the larger stability of 3. The 9.4 kcal/mol of energy difference between 3 and 4 comes mainly from the interaction energy (ΔE_{int}) that is 10.5 kcal/mol lower in 3. More stabilizing ΔE_{int} energy for 3 is the result of better electrostatic (9.0 kcal/mol) and orbital interaction (29.6 kcal/mol) components. Again, the more stabilizing ΔV_{elstat} term in 3 can be understood by taking into account that in this isomer the dipole moments of the fragments are placed in a better orientation to favor the electrostatic interactions. The absolute value of the energy associated to the ΔV_{elstat} term is higher than in the diazacyclobutadiene isomers since larger fragments usually produce higher Pauli repulsions and electrostatic interactions. In addition, the dipole moment of the 1-azapropendiyl fragment is somewhat larger than that of the azaethynyl fragment (1.626 and 2.450 D for A(4) and B(4), respectively). Decomposition of ΔE_{oi} into σ and π components (ΔE_{σ} and ΔE_{π}) shows that ΔE_{π} is much larger in aromatic pyrazole and imidazole rings than in the previous antiaromatic diazacyclobutadiene compounds. This is in agreement with the results reported by Frenking et al. in a series of aromatic and antiaromatic organic compounds.³⁷ This ΔE_{π} component is almost the same for the two compounds, in agreement with the similar strength of the C=C, C=N, and N=N double bonds,²⁰ yet somewhat larger for 4 in line with the results obtained from aromaticity indicators (vide supra). As in the diazacyclobutadiene isomers, ΔE_{σ} represents the main contribution (30.3 kcal/mol) to the higher stability of the imidazole isomer and comes from the larger energy release in the formation of two C–N bonds as compared to the constitution of C–C and N–N bonds.

Following the same procedure, we have constructed a deformed pyrazole ring (4a) from A(3) + B(3) fragments but with connecting N–N and C–C bond distances equal to the

corresponding C–N bond lengths in 3. In this way, 3 and 4a are exactly the same compound but just with an A(3) fragment turned upside down in 4a. As compared to 4, 4a is 9.7 kcal/mol less stable and the difference comes basically from a small increase in the Pauli repulsion that is not compensated by the concomitant increase in electrostatic interactions. The most important conclusion from this analysis is that the Pauli repulsion is more important in imidazole than pyrazole and cannot be used to explain the higher stability of the former. In the last step, we move from 4a to 4b, the latter being a deformed pyrazole ring generated from A(3) + B(3) fragments but with connecting N–N and C–C bond distances equal to the corresponding bond lengths in 4. Somewhat unexpectedly, 4b is slightly less stable than 4a, and this is due to the larger root-mean-square deviations (rmsd) found for the five angles of 4 in 4b ($\text{rmsd} = (\sum_{i=1}^5 (\theta_i^{\text{a/b}} - \theta_i^{\text{a}})^2/5)^{1/2} = 7.0^\circ$) as compared to 4a ($\text{rmsd} = 5.9^\circ$). Again, the main changes correspond to the Pauli repulsions and electrostatic interactions that come closer to the values in 4 from A(4) + B(4) fragments. Finally, we have calculated (BP86/aug-cc-pVTZ//BP86/TZ2P results with the QTAIM partition) the delocalization index ($\delta(\text{A,B})$) of the N–N bonds in pyrazole (1.383), *trans*-hydrazine (1.222), and *trans*-diazene (2.182). From these numbers, we have made a rough estimation of the percentage of the pyrazole resonant structure having a N=N double bond (17%) and that having a N–N single bond (83%). Clearly, the latter is the dominant for this species.

3.3. 1,2- and 1,3-Diazines. The optimized geometries obtained at the BP86/TZ2P level of the closed-shell singlet ground state of pyridazine and pyrimidine rings are depicted in Figure 1. Their molecular structures and the experimental values^{61,62} are very similar, differences in bond lengths being about one hundredth of an angstrom and in the angles of one tenth of a degree. It is worth noting that NN and CN bonds in these two diazine isomers are about 0.05 Å shorter than the CC bonds, despite the fact that the latter are stronger. This has been already discussed in detail by Bickelhaupt et al.⁴⁷ in the study of the bonding mechanism in the CN dimers, and, basically, it is the consequence of the SOMO orbital on the N fragment involved in the formation of the σ C–N and N–N bonds being more contracted than that on the C fragment. Thus, CN and especially NN bond lengths have to shorten to reach good SOMO–SOMO overlap at the cost of higher Pauli repulsions. All angles are around the expected 120°. Pyrimidine is 20.9 kcal/mol more stable than pyridazine at the BP86/TZ2P

level (22.7 kcal/mol at CCSD(T)/aug-cc-pVTZ//BP86/TZ2P level of theory) close to the experimental value of 19.7 kcal/mol determined from enthalpies of combustion.¹² The isomerization energy in this case is the largest among the three rings studied. As compared to 1,2- and 1,3-azoles, this is in part due to the partial H-bond formed in pyrazole that stabilizes somewhat this molecule with respect to imidazole. Such stabilization is not present in pyridazine. As in the case of azoles, the isomerization energy cannot be attributed to a different aromaticity of the two rings. Indeed, most aromaticity indices analyzed (resonance energies,^{19,20,63} HOMA,^{58,60} Bird index,^{18,19,64} NICS,^{20,58,60,65} ring currents,^{65,66} PDI,⁶⁰ FLU,⁶⁰ and multicenter indices^{42,56,58,60}) point out a similar aromaticity of the two rings, although in most of the cases pyridazine with the NN bond is considered slightly more aromatic. The reason for the higher stability of pyrimidine can be discussed from the results of the EDA of pyrimidine (**5**) and pyridazine (**6**) generated from azaethendiyl A and 1-azabutendiyl C fragments, both in their triplet states (see Table 4). As before, the fragments A and C that can be obtained from **5** and **6** are slightly different and, therefore, **5** and **6** can be generated using fragments derived from **5** (A(**5**) and C(**5**)) fragments, or originated from **6** (A(**6**) + C(**6**)).

The comparison between the EDA of pyrimidine and pyridazine leads to similar conclusions as in the previously studied isomers. First, deformation energy almost does not contribute to the isomerization energy; second, Pauli repulsion favors the isomer with the NN bond because the larger Pauli repulsion in the formation of the N–N bond is compensated by a low Pauli repulsion of the C–C bond; third, electrostatic interactions favor the compound with new formed C–N bonds; and finally, orbital interactions are more stabilizing in the formation of two new σ C–N bonds than in the generation of σ C–C and N–N bonds (the π component does not introduce major differences). Interestingly, the ΔE_{π} component in compounds **5** and **6** is the largest among the different isomers analyzed in this study, as expected from the larger aromaticity of these compounds. It is worth noting that the ΔE_{σ} component increases gradually from the diazacyclobutadienes to the diazines as a result of increased SOMO overlaps due to better orientations (ring angles become larger) together with the increased polarization in larger fragments. When the deformed pyridazine **6a** is formed with frozen A(**5**) and C(**5**) fragments but with connecting N–N and C–C bond distances as the corresponding C–N bond lengths in **5**, it is found that, as compared to **6**, the Pauli repulsion increases but still is lower than that of **5** and the stabilization due to electrostatic interactions and orbital interactions is reduced. Overall, the energy difference between **6a** and **5** is 28.3 kcal/mol. It is worth noting that in **6a** the ΔE_{π} component is slightly more stabilizing than in **5**, in line with the fact that most aromaticity descriptors find pyridazine somewhat more aromatic than pyrimidine. Finally, the deformed pyridazine **6b**, which is pyridazine with frozen A(**5**) and C(**5**) fragments but with connecting N–N and C–C bond distances as the optimized bond lengths in **6**, represents an intermediate situation between **6** and **6a**. Finally, as before, we have calculated $\delta(\text{N,N})$ for pyridazine (1.526) to estimate the percentage of the resonant structure in pyridazine having a double N=N and that having a single N–N bond. Again, the latter with a 68% is the dominant structure.

To conclude, we emphasize the relatively large Pauli repulsion values in the systems analyzed, especially those of pyrazole/imidazole (593.3 and 621.5 kcal mol⁻¹) and

pyridazine/pyrimidine (735.8 and 814.1 kcal mol⁻¹). A pertinent comparison could be made with the EDA results obtained for diatomic N₂,⁶⁷ which has a Pauli repulsion (802.4 kcal mol⁻¹) only from the σ -electrons, but none from π -electrons. Pauli repulsion in σ -bonds is much larger than Pauli repulsion from lone pairs, because of the (avoided) overlap of the lone-pair orbitals.

4. CONCLUSIONS

In this work, we have analyzed using a Morokuma-like energy decomposition analysis and the turn-upside-down approach the isomerization energies of 1,2- and 1,3-diazacyclobutadiene, pyrazole and imidazole, and pyrimidine and pyridazine. In all cases, the 1,3-isomer has been found to be more stable than the 1,2-counterpart. Our main conclusion is that, although the large Pauli repulsion (together with some polarization effects) explains the weaker N–N bond, it does not account for the higher stability of the 1,3-isomers studied in this work. The 1,2-isomers have, in fact, a lower Pauli repulsion than the 1,3-forms, which are more stable not because a lower Pauli repulsion of the two C–N bonds as compared to the C–C and N–N bonds, but due to the more favorable electrostatics and σ -orbital interactions involved in the formation of two C–N bonds in comparison with the generation of C–C and N–N bonds in 1,2-isomers.

■ ASSOCIATED CONTENT

📄 Supporting Information

Figures S1 and S2 depict EDA results for CC, CN, and NN σ -bonds in CH₃–CH₃, CH₃–NH₂, and *cis*-NH₂–NH₂ in their eclipsed conformation. Table S1 containing the Cartesian coordinates and energies of all optimized species. This material is available free of charge via the Internet at <http://pubs.acs.org>.

■ AUTHOR INFORMATION

Corresponding Author

*E-mail: (J.P.) jordi.poater@udg.edu; (M.S.) miquel.sola@udg.edu

■ ACKNOWLEDGMENTS

We thank the following organizations for financial support: the Ministerio de Ciencia e Innovación (MICINN, Project Nos. CTQ2008-03077/BQU, CTQ2008-06532/BQU, and CTQ2011-23156/BQU, Ramón y Cajal contract to J.P., and FPI fellowship to M.E.H.) and the DIUE of the Generalitat de Catalunya (project no. 2009SGR637). W.T. thanks FONDECYT (Grant No. 1109043). We acknowledge helpful comments from Prof. Dr. F. Matthias Bickelhaupt. Excellent service by the Centre de Supercomputació de Catalunya (CESCA) is gratefully acknowledged. Support for the research of M.S. was received through the ICREA Academia 2009 prize for excellence in research funded by the DIUE of the Generalitat de Catalunya.

■ REFERENCES

- (1) Poater, J.; Visser, R.; Solà, M.; Bickelhaupt, F. M. *J. Org. Chem.* **2007**, *72*, 1134.
- (2) Kitaura, K.; Morokuma, K. *Int. J. Quantum Chem.* **1976**, *10*, 325. Morokuma, K. *Acc. Chem. Res.* **1977**, *10*, 294.
- (3) Matta, C. F.; Hernández-Trujillo, J.; Tang, T.-H.; Bader, R. F. W. *Chem.—Eur. J.* **2003**, *9*, 1940.
- (4) Grimme, S.; Mück-Lichtenfeld, C.; Erker, G.; Kehr, G.; Wang, H.; Beckers, H.; Willner, H. *Angew. Chem., Int. Ed.* **2009**, *48*, 2592.

- (5) Eicher, T.; Hauptmann, S. *The Chemistry of Heterocycles*; John Wiley & Sons: Chichester, 2003. Katritzky, A. R.; Jug, K.; Oniciu, D. C. *Chem. Rev.* **2001**, *101*, 1421.
- (6) *Comprehensive Heterocyclic Chemistry III*; Katritzky, A. R., Ramsden, C. A., Scriven, E. F. V., Taylor, R. J. K., Eds.; Elsevier: Amsterdam, 2008; Vol. 2. *Chemistry of Heterocyclic Compounds: Small Ring Heterocycles*; Hassner, A., Ed.; Wiley: New York, 2008; Vol. 42.
- (7) Pavlik, J. W.; Changtong, C.; Tsefrikas, V. M. *J. Org. Chem.* **2003**, *68*, 4855. King, D. S.; Denny, C. T.; Hochstrasser, R. M.; Smith, A. B. III. *J. Am. Chem. Soc.* **1977**, *99*, 271.
- (8) Deng, S.; Schwarzmaier, C.; Zabel, M.; Nixon, J. F.; Bodensteiner, M.; Peresyphkina, E. V.; Balázs, G.; Scheer, M. *Eur. J. Inorg. Chem.* **2011**, 2991.
- (9) Politzer, P.; Grice, M. E.; Murray, J. S.; Seminario, J. M. *Can. J. Chem.* **1993**, *71*, 1123.
- (10) Brown, E. G. *Ring Nitrogen and Key Biomolecules. The Biochemistry of N-heterocycles*; Kluwer Academic Press: Dordrecht, 1998.
- (11) Schmidt, A.; Dreger, A. *Curr. Org. Chem.* **2011**, *15*, 1423. Kini, S.; Gandhi, A. M. *Indian J. Pharm. Sci.* **2008**, *70*, 105.
- (12) Tjebbes, J. *Acta Chem. Scand.* **1962**, *16*, 916.
- (13) da Silva, G.; Moore, E. E.; Bozzelli, J. W. *J. Phys. Chem. A* **2006**, *110*, 13979.
- (14) Bedford, A. F.; Edmondson, P. B.; Mortimer, C. T. *J. Chem. Soc.* **1962**, 2927.
- (15) Jiménez, P.; Roux, M. V.; Turrión, C.; Gomis, F. *J. Chem. Thermodyn.* **1987**, *19*, 985.
- (16) Curutchet, C.; Poater, J.; Solà, M.; Elguero, J. *J. Phys. Chem. A* **2011**, *111*, 8571.
- (17) Glukhovtsev, M. N.; Simkin, B. Y.; Minkin, V. I. *J. Struct. Chem.* **1987**, *28*, 483.
- (18) Bird, C. W. *Tetrahedron* **1996**, *52*, 9945.
- (19) Bird, C. W. *Tetrahedron* **1997**, *53*, 13111.
- (20) Wang, Y.; Wu, J. I.-C.; Li, Q.; Schleyer, P. v. R. *Org. Lett.* **2010**, *12*, 4824.
- (21) Baerends, E. J.; Autschbach, J.; Bérces, A.; Bickelhaupt, F. M.; Bo, C.; de Boeij, P. L.; Boerrigter, P. M.; Cavallo, L.; Chong, D. P.; Deng, L.; Dickson, R. M.; Ellis, D. E.; Fan, L.; Fischer, T. H.; Fonseca Guerra, C.; van Gisbergen, S. J. A.; Groeneveld, J. A.; Gritsenko, O. V.; Grüning, M.; Harris, F. E.; van den Hoek, P.; Jacob, C. R.; Jacobsen, H.; Jensen, L.; van Kessel, G.; Kootstra, F.; van Lenthe, E.; McCormack, D. A.; Michalak, A.; Neugebauer, J.; Osinga, V. P.; Patchkovskii, S.; Philipsen, P. H. T.; Post, D.; Pye, C. C.; Ravenek, W.; Ros, P.; Schipper, P. R. T.; Schreckenbach, G.; Snijders, J. G.; Solà, M.; Swart, M.; Swerhone, D.; te Velde, G.; Vernooijs, P.; Versluis, L.; Visscher, L.; Visser, O.; Wang, F.; Wesolowski, T. A.; van Wezenbeek, E.; Wiesenekker, G.; Wolff, S. K.; Woo, T. K.; Yakovlev, A. L.; Ziegler, T. *Amsterdam Density Functional*, Amsterdam, 2006.
- (22) te Velde, G.; Bickelhaupt, F. M.; Baerends, E. J.; Fonseca Guerra, C.; van Gisbergen, S. J. A.; Snijders, J. G.; Ziegler, T. *J. Comput. Chem.* **2001**, *22*, 931.
- (23) Snijders, J. G.; Baerends, E. J.; Vernooijs, P. *At. Nucl. Data Tables* **1981**, *26*, 483.
- (24) Swart, M.; Snijders, J. G. *Theor. Chem. Acc.* **2003**, *110*, 34.
- (25) Baerends, E. J.; Ellis, D. E.; Ros, P. *Chem. Phys.* **1973**, *2*, 41.
- (26) Vosko, S. H.; Wilk, L.; Nusair, M. *Can. J. Phys.* **1980**, *58*, 1200.
- (27) Becke, A. D. *Phys. Rev. A* **1988**, *38*, 3098.
- (28) Perdew, J. P. *Phys. Rev. B* **1986**, *33*, 8800.
- (29) Atkins, P.; De Paula, J. *Physical Chemistry*; Oxford University Press: Oxford, 2006.
- (30) Frisch, M. J.; Trucks, G. W.; Schlegel, H. B.; Scuseria, G. E.; Robb, M. A.; Cheeseman, J. R.; Scalmani, G.; Barone, V.; Mennucci, B.; Petersson, G. A.; Nakatsuji, H.; Caricato, M.; Li, X.; Hratchian, H. P.; Izmaylov, A. F.; Bloino, J.; Zheng, G.; Sonnenberg, J. L.; Hada, M.; Ehara, M.; Toyota, K.; Fukuda, R.; Hasegawa, J.; Ishida, M.; Nakajima, T.; Honda, Y.; Kitao, O.; Nakai, H.; Vreven, T.; Montgomery, J. A., Jr.; Peralta, J. E.; Ogliaro, F.; Bearpark, M.; Heyd, J. J.; Brothers, E.; Kudin, K. N.; Staroverov, V. N.; Kobayashi, R.; Normand, J.; Raghavachari, K.; Rendell, A.; Burant, J. C.; Iyengar, S. S.; Tomasi, J.; Cossi, M.; Rega, N.; Millam, J. M.; Klene, M.; Knox, J. E.; Cross, J. B.; Bakken, V.; Adamo, C.; Jaramillo, J.; Gomperts, R.; Stratmann, R. E.; Yazyev, O.; Austin, A. J.; Cammi, R.; Pomelli, C.; Ochterski, J. W.; Martin, R. L.; Morokuma, K.; Zakrzewski, V. G.; Voth, G. A.; Salvador, P.; Dannenberg, J. J.; Dapprich, S.; Daniels, A. D.; Farkas, Ö.; Foresman, J. B.; Ortiz, J. V.; Cioslowski, J.; Fox, D. J. *Gaussian 09*, Revision A.02; Gaussian, Inc.: Pittsburgh, PA, 2009.
- (31) Cizek, J. *J. Chem. Phys.* **1966**, *45*, 4256.
- (32) Purvis, G. D. III; Bartlett, R. J. *J. Chem. Phys.* **1982**, *76*, 1910.
- (33) Raghavachari, K.; Trucks, G. W.; Pople, J. A.; Head-Gordon, M. *Chem. Phys. Lett.* **1989**, *157*, 479.
- (34) Dunning, T. H. Jr. *J. Chem. Phys.* **1989**, *90*, 1007. Kendall, R. A.; Dunning, T. H. Jr.; Harrison, R. J. *J. Chem. Phys.* **1992**, *96*, 6796.
- (35) Bickelhaupt, F. M.; Baerends, E. J.; Lipkowitz, K. B.; Boyd, D. B., Eds. Wiley-VCH: New York, 2000; Vol. 15, p 1. Morokuma, K. *Acc. Chem. Res.* **1977**, *10*, 294.
- (36) Ziegler, T.; Rauk, A. *Theor. Chim. Acta* **1977**, *46*, 1. Ziegler, T.; Rauk, A. *Inorg. Chem.* **1979**, *18*, 1558.
- (37) Fernández, I.; Frenking, G. *Faraday Discuss.* **2007**, *135*, 403.
- (38) Fernández, I.; Frenking, G. *Chem.—Eur. J.* **2007**, *13*, 5873.
- (39) Jursic, B. S. *J. Mol. Struct., THEOCHEM* **2001**, *536*, 143.
- (40) Chen, Z.; Wannere, C. S.; Corminboeuf, F.; Puchta, R.; Schleyer, P. v. R. *Chem. Rev.* **2005**, *105*, 3842. Schleyer, P. v. R.; Maerker, C.; Dransfeld, A.; Jiao, H.; van Eikema Hommes, N. J. R. *J. Am. Chem. Soc.* **1996**, *118*, 6317.
- (41) Matito, E.; Duran, M.; Solà, M. *J. Chem. Phys.* **2005**, *122*, 014109. Matito, E.; Duran, M.; Solà, M. *J. Chem. Phys.* **2006**, *125*, 059901.
- (42) Giambiagi, M.; de Giambiagi, M. S.; dos Santos Silva, C. D.; de Figueiredo, A. P. *Phys. Chem. Chem. Phys.* **2000**, *2*, 3381.
- (43) Bultinck, P.; Ponec, R.; Van Damme, S. *J. Phys. Org. Chem.* **2005**, *18*, 706.
- (44) Alonso, M.; Poater, J.; Solà, M. *Struct. Chem.* **2007**, *18*, 773. Feixas, F.; Matito, E.; Solà, M.; Poater, J. *Phys. Chem. Chem. Phys.* **2010**, *12*, 7126.
- (45) Schaad, L. J.; Hess, B. A. Jr. *Chem. Rev.* **2001**, *101*, 1465.
- (46) van Zeist, W.-J.; Bickelhaupt, F. M. *Phys. Chem. Chem. Phys.* **2009**, *11*, 10317.
- (47) Bickelhaupt, F. M.; Nibbering, N. M. M.; van Wezenbeek, E. M.; Baerends, E. J. *J. Phys. Chem.* **1992**, *96*, 4864.
- (48) Nygaard, L.; Christen, D.; Nielsen, J. T.; Pedersen, E. J.; Snerling, O.; Vestergaard, E.; Sørensen, G. O. *J. Mol. Struct.* **1974**, *22*, 401.
- (49) Christen, D.; Griffiths, J. H.; Sheridan, J. Z. *Naturforsch. A* **1982**, *36*, 1378.
- (50) Krygowski, T. M.; Oziminski, W. P.; Ramsden, C. A. *J. Mol. Model* **2011**, *17*, 1427.
- (51) Cyrański, M. K.; Schleyer, P. v. R.; Krygowski, T. M.; Jiao, H.; Hohlneicher, G. *Tetrahedron* **2003**, *59*, 1657.
- (52) Cyrański, M. K.; Krygowski, T. M.; Katritzky, A. R.; Schleyer, P. v. R. *J. Org. Chem.* **2002**, *67*, 1333.
- (53) Cyrański, M. K. *Chem. Rev.* **2005**, *105*, 3773.
- (54) Kotelevskii, S. I.; Prezhdo, O. V. *Tetrahedron* **2001**, *57*, 5715.
- (55) Bird, C. W. *Tetrahedron* **1985**, *41*, 1409.
- (56) Mandado, M.; Otero, N.; Mosquera, R. A. *Tetrahedron* **2006**, *62*, 12204.
- (57) Bean, G. P. *J. Org. Chem.* **1998**, *63*, 2497.
- (58) Mandado, M.; González-Moa, M. J.; Mosquera, R. A. *J. Comput. Chem.* **2007**, *28*, 127.
- (59) Matito, E.; Poater, J.; Solà, M.; Schleyer, P. v. R. In *Chemical Reactivity Theory*; Chattaraj, P. K., Ed.; Taylor and Francis/CRC Press: Boca Raton, 2009; p 419. Havenith, R. W. A.; Jiao, H.; Jenneskens, L. W.; van Lenthe, J. H.; Sarobe, M.; Schleyer, P. v. R.; Kataoka, M.; Necula, A.; Scott, L. T. *J. Am. Chem. Soc.* **2002**, *124*, 2363.
- (60) Feixas, F.; Matito, E.; Poater, J.; Solà, M. *J. Comput. Chem.* **2008**, *29*, 1543.
- (61) Jorgensen, W. L.; McDonald, N. A. *J. Mol. Struct., THEOCHEM* **1998**, *424*, 145.

- (62) Cradock, S.; Liescheski, P. B.; Rankin, D. W. H.; Robertson, H. *E. J. Am. Chem. Soc.* **1988**, *110*, 2758.
- (63) Wiberg, K. B. *J. Am. Chem. Soc.* **1989**, *111*, 4178.
- (64) Fabian, J.; Lewars, E. *Can. J. Chem.* **2004**, *82*, 50.
- (65) Stanger, A. *J. Org. Chem.* **2010**, *75*, 2281.
- (66) Amusooya, Y.; Chakrabarti, A.; Patti, S. K.; Ramasesha, S. *Int. J. Quantum Chem.* **1998**, *70*, 503.
- (67) Krapp, A.; Bickelhaupt, F. M.; Frenking, G. *Chem.—Eur. J.* **2006**, *12*, 9196.